Projecting Salt Intrusion in the Rhine-Meuse Delta using CNN-based reconstructed discharge

MSc Thesis by Jesse Koppenaal

Supervised by Henk Dijkstra and Huib de Swart

In collaboration with Jiyong Lee and Bouke Biemond

Institute for Marine and Atmospheric Sciences, Utrecht University

Key Points:

- We project the impact of climate change-induced river discharge perturbations on Salt Intrusion in the Rhine-Meuse Delta.
- Future discharge is reconstructed from forcing conditions using a machine learning approach and converted to Salt Intrusion Length with an idealized hydrological model.
- Future Salt Intrusion events are projected to be more frequent by the end of the century under SSP5-8.5, while the frequency remains constant under SSP2-4.5.

Corresponding author: Jesse Koppenaal, jesse.koppenaal@gmail.com

Abstract
This research projects future salt intrusion in the Rhine-Meuse Delta (RMD) based on forcing in the CMIP6 simulations. This is achieved using a Convolutional Neural Network (CNN) to reconstruct river discharge from meteorological forcing conditions, and calculating salt intrusion statistics with an idealized model (IMSIDE). The CNN is trained on the ERA5 reanalysis product and observational discharge data and subsequently applied to forcing data from the ScenarioMIP product under Shared Socioeconomic Pathways SSP2-4.5 and SSP5-8.5. The resulting discharge projections are used as forcing of IMSIDE to provide estimates of future salt intrusion lengths (SIL) in the RMD. Results indicate an increase in both frequency and intensity of salt intrusion events under the higher emission scenario SSP5-8.5. No significant changes in SIL are projected under the moderate emission scenario SSP2-4.5. The presence of biases in CMIP6 projections as well as CNN underprediction of discharge in the dry season effect discharge projections and the resulting SIL statistics.

Plain Language Summary

The Rhine-Meuse Delta in the Netherlands is vulnerable to saltwater moving inland, which can affect agriculture, industry, and ecosystems. In this research, an AI model is used to predict river discharge based on future climate conditions. Estimations are made on how far and how often saltwater will travel inland by the end of this century, based on the long-term change in river discharge. We find that the frequency of saltwater intrusion will increase under a high emission scenario, while no change is shown for a moderate emission scenario.

1 Introduction

The Rhine-Meuse Delta (RMD) is densely populated and highly susceptible to increasing saline water intrusion (van Den Brink et al., 2019). Along the delta many agricultural, industrial and biological aspects depend heavily on the availability of fresh water in this region(Klijn et al., 2012). It has long been understood that a changing climate will increase risk of extreme salt intrusion. (Jacobs et al., 2000) The main drivers of this increasing risk are Sea Level Rise (SLR) and decreasing river discharge, both of which cause saline water to penetrate further upstream and with greater frequency (Savenije, 2012). A recent study on other the Po river shows that decreased freshwater discharge under prolonged droughts is the dominant effect there, while SLR has a less significant impact (Bellafiore et al., 2021). Furthermore, an empirical relation between Salt Intrusion Length (SIL) and river discharge has been used for practical water management purposes (Monismith et al., 2002). Conversely SLR has been identified as the main feature of increased salt intrusion in two Portuguese estuaries (Pereira et al., 2022). Both factors have been found to be vital in the case of the Rhine-Meuse Delta considered in this study (van Den Brink et al., 2019). This study is aimed towards quantifying the effect of long-term discharge change on salt intrusion in particular. Under any climate change scenario, river discharge in the Rhine-Meuse basin has been shown to increase in winter but strongly decrease in summer, especially under SSP5-8.5 (Buitink et al., 2023). The focus of this study will be on the effect of future discharge on SIL statistics, where a Convolutional Neural Network (CNN) is used to obtain discharge projections.

The data-driven machine learning approach of discharge reconstruction is promising due to its effectiveness with non-linear systems (Tran et al., 2015). This approach also benefits from favourable runtime, in this study about a minute for 85 years of daily steps. In the context of hydrological extremes, it has outperformed traditional methods for discharge prediction tasks (Hauswirth et al., 2021). However, applying it to the RMD's complex river network has been challenging due to its multi-branch nature and human management (Wullems et al., 2023). In order to use machine learning exclusively to its strengths, the task of SIL projections is split into two distinct steps.

The first step is to reconstruct river discharge from forcing conditions, where the CNN is used for fast and accurate assessments. To accurately assess the future frequency and intensity of such events and obtain meaningful statistics, river discharge has to be studied at a high temporal resolution. As of today most Global Circulation Models (GCM's) do not include river discharge on a daily resolution, with a notable exception being CESM-LE2 which has daily discharge for SSP3 (Lee et al., 2024). Furthermore discharge is a grid-based quantity in GCM's, which can induce a mismatch between the model output and the practical river-based water management issues. This mismatch is especially present when the scale of the projections (100 km for CMIP6) is substantially larger than the scale of individual river catchments. Several approaches have been explored to tackle this like applying a hydrological model to the raw GCM forcing (Buitink et al., 2023) or using Regional Climate Models with have a finer resolution (Dadson et al., 2011). Discharge obtained through this methodology can be incorporated in the output of GCM's to increase their practical applicability in this respect.

The second step concerns obtaining the salt intrusion projections using the CNN-predicted discharge series. Here an idealized hydrological model is used which explicitly takes the complex river network of the Delta into account (Biemond et al., 2022). This model solves the salinity balance of the network structure of the RMD using a balance between downstream salt transport due to the river flow and upstream salt transport due to exchange flow, tidal flow and horizontal tide-induced mixing. It also solves for the interaction between the different branches of the RMD network. Based on the balance between upstream and downstream fluxes the Salt Intrusion Length (SIL) is determined, here quantified as the distance between 2−psu isohaline and the estuary mouth X_2 (Monismith et al., 2002). In studies with a broader scope the X_2 has been calculated using an idealized sub-tidal model solving cross-sectionally averaged equations for hydrodynamics and the salt budget (Lee et al., 2024; Chen, 2015).

In this study, the effect of change in discharge on future salt intrusion time series is quantified using a CNN combined with a hydrological model. The CNN is trained on meteorological forcing data from the ERA5 reanalysis product combined with observational discharge data from Rijkswaterstaat (RWS). The trained model is applied to CMIP6 forcing projections to obtain discharge projections for the Rhine and Meuse rivers, as these make up the essential input for IMSIDE runs. Projections for future salt intrusion are then obtained from the river discharge results using IMSIDE for salt intrusion in the RMD. To investigate the systems sensitivity to climate change signal, forcing outputs are used for both SSP2-4.5 and SSP5-8.5 and the resulting statistics of SIL is evaluated.

2 Methods

A machine learning model is designed to reconstruct current river discharge from meteorological forcing conditions, using which projections for future salt intrusion events are obtained. First an outline is given of the relevant study area and the precise stations for which the reconstruction of discharge is performed (Section 2.1). The setup of the CNN is outlined in along with the training and evaluation method using ERA5 reanalysis data (Section 2.2). Next the CNN is applied to CMIP6 model data to obtain future discharge projections, along with a skill evaluation on the historical period (Section 2.3). Finally, the obtained river discharges are fed into IMSIDE to obtain future projections of salt intrusion in the Rhine-Meuse Delta (Section 2.4).

Figure 1. Schematic overview of the Rhine-Meuse Delta and the distribution of river discharge between its constituents. (*M. Dörrbecker*, 2019)

2.1 Study Area

The RMD consists of a complex network of rivers, weirs and channels. It originates mainly from the Rhine river, flowing into the Netherlands in the east of the country. The Rhine branches off into the Waal and Lek while the Meuse which reach the estuarine region of the RMD separately. The Meuse enters the country in the southern most province near Maastricht and flows parallel to the Waal up to the delta region. The Delta culminates in the Rotterdam urban area where it connects to the North Sea through the Nieuwe Waterweg as well as the Haringvliet sluice. The northern part of the RMD consists of two main waterways, the Nieuwe Maas and Oude Maas. Intrusion of saline water is driven here by estuarine circulation as well as tidal mixing processes (de Nijs & Pietrzak, 2012). River discharge is predicted for downstream stations Tiel and Megen using meteorological data of the entire basin of the Rhine and Meuse respectively. These stations are chosen to ensure compatibility with IMSIDE. The Meuse originates in France and flows through Belgium and into the Netherlands where it connects to the RMD. The Rhine has many sources, the most important of which is located in the Alps of Switzerland and from there flows mainly through the German Rhineland. To accurately assess the river discharge near the Dutch border the entire Rhine Basin must be taken into account, including major tributaries like the Aare, Main and Neckar (Uehlinger et al., 2009).

Table 1. Variables used in training the CNN to reconstruct discharge from forcing conditions. This overview applies to the training process only, as CMIP6 forcing is used in the remainder of this study.

Variable	Unit	Source	Resolution	Frequency
Precipitation (P)	mm	ERA5	1 degree	daily
Temperature (T)	K	ERA5	1 degree	daily
Volumetric Soil Water (VSW)	m^3/m^3	ERA5	1 degree	daily
Discharge (Q)	m^3s^{-1}	RWS	point	daily

2.2 CNN Setup And Validation

A Convolutional Neural Network (CNN) is used to downscale meteorological forcing conditions to river discharge output.The CNN uses time series of spatial maps of key variable as its features while the labels are observational discharge data measured at the Tiel and Megen station of the Rhine and Meuse river, respectively. For the CNN to parse 3D (t, x, y) data in each of its layers, Conv3D layers are used as they have been shown to be able to capture spatiotemporal trends to a high degree (Sun et al., 2021; Tran et al., 2015). The network's weights are trained using the ERA5 reanalysis dataset as features (Hersbach et al., 2020), while labels are discharge measurements obtained from Rijkswaterstaat (RWS) (Rijkswaterstaat, 2024). The data is split into a training (2001-2012), validation (2013-2015) and test (2016-2020) to be able to evaluate model performance on the ERA5 set. After hyperparameter tuning is done by considering the performance on the validation test, the final model's weights are saved to be used on CMIP6 projections. The test set is used for a final evaluation of the model skill only. To quantify model predictive strength the Kling-Gupta Efficiency (KGE) (Knoben et al., 2019) is calculated.

Given the size of the RM basin, river discharge at downstream station will exhibit a delayed response to forcing conditions in the upstream areas. The amount of time delay in the response is quantified by calculating the correlation between river discharge and the precipitation in the full basin. For the Rhine the time delay is set to 40 days while the Meuse uses a 20 day response time based on this correlation (Supplemental Information). A mask with values -1 is applied to all cells within the grid that are not close to any branch of the relevant river basin, so that the CNN will not take these areas into account and therefor converge its weights more rapidly.

More details on the CNN setup and validation can be found in the Supplemental Information.

2.3 Applying CNN To CMIP6

The CNN trained on ERA5 reanalysis data is saved and now applied to CMIP6 climate projections in order to obtain future time series of discharge at the Tiel and Megen station. Projections for future forcing conditions are obtained from the ScenarioMIP product of the CMIP6 dataset. Members included in this research are selected by the availability of the relevant forcing conditions at the required temporal and spatial resolution. Specifically this means a 1 degree spatial resolution as well as a temporal resolution of one day. The other critical selection criteria is the availability of ScenarioMIP runs for different Shared Socioeconomic Pathways (SSP) (O'Neill et al., 2016). Finally, the members must include the variable $mrsos$ (alongside precipitation and near-surface temperature, which are present in every set), which is defined as the soil moisture up to a depth of $10cm$. This variable is analogous to the VSW variable in the ERA5 reanalysis set, which represents the volumetric soil wetness up to a depth of $7cm$. To convert the CMIP6 $mrsos$ data to fit the VSW variable on which the CNN is trained, it is assumed that the soil moisture within the upper layer is evenly distributed, as in (Qiao et al., 2022). We find that this parameter is crucial for the CNN performance in terms of discharge reconstruction. (Supplemental Information)

Selected members based on these criteria are CESM (Danabasoglu et al., 2020), NorESM (Seland et al., 2020), CMCC (Lovato et al., 2022), EC-Earth (Döscher et al., 2021) and MRI (Yukimoto et al., 2019). Data is obtained for both SSP2-4.5 and SSP5-8.5 as part of the ScenarioMIP output. The raw data is linearly interpolated to fit the exact 1x1 degree grid used by the CNN, to make sure that the input is consistent with that of the ERA5 training set. Furthermore the precipitation and volumetric soil content data is transformed to match the unit of the ERA5 dataset on which the CNN is trained. The CMIP6 data is normalized using normalisation which is fitted to ERA5 data during model training, to ensure consistent predictions.

Application of the CNN to the CMIP6 model output yields time series of river discharge for the entirety of the CMIP6 model runs, which consists of the period 2015-2099. The process of training the CNN, saving the fitted normalisation settings and obtaining river discharge from CMIP6 is done separately for the Rhine and Meuse basin. An estimate of model performance is obtained by comparing the CNN-predicted discharge of the historical part of the data to the observational discharge measured at the corresponding stations.

2.4 Projecting Future SIL

The future discharge projections are obtained for the station Tiel and Megen for the Rhine and Meuse river respectively. These two time series are used as input for IMSIDE to produce time series of SIL (X_2) in the Rhine-Meuse basin.

IMSIDE is an idealized hydrological model which resolves the salt balance using width-averaged river flow and salinity. The model takes into account the contributions from mean discharge, density-driven flow and the $M2$ tidal mode in a channel network. The transport quantities of salt are calculated using an advection-diffusion equation based on these physical processes. (Supplemental Information) To obtain SIL statistics this equation is solved using a decomposition in depth-averaged and depth-dependent flow velocity and salinity. IMSIDE takes into account the network of rivers, weirs and canals of the Rhine-Meuse Delta. In particular the interaction at each junction of the network is calculated by solving the salt and discharge balances at the intersection (Biemond et al., 2023). The model output used in this study are time series of SIL at the Nieuwe Maas and Oude Maas channels.

Alongside the Tiel and Megen discharge IMSIDE also requires a time series of discharge at three additional points: Lek, Hollandsche IJssel and Haringvliet. For the purposes of this research these are all set to zero. This is based on the assumption that in the summer months crucial for SI, these discharges will be small compared to the Tiel and Megen discharge (Huismans et al., 2017). Additionally, the excess water volume brought into the system through Hollandse IJssel and Lek will be largely compensated by the additional outflow at Haringvliet.

Time series of SIL are obtained through IMSIDE for the Nieuwe Maas and Oude Maas waterways, for the 5 CMIP members and scenario's SSP2-4.5 and SSP5-8.5. The resulting PDF's are compared to examine the system's response to climate change, its sensitivity to the differences in emission scenario's, as well as the ensemble spread. SIL statistics are quantified by analysing the PDF of X_2 in the most relevant season for salt intrusion, which are the months August, September and October (Klijn et al., 2012). This is also reflected in Figure 3 where the lowest observed discharge is found to be in these months. The X_2 PDF is calculated for a baseline period 2015-2045 as well as a future

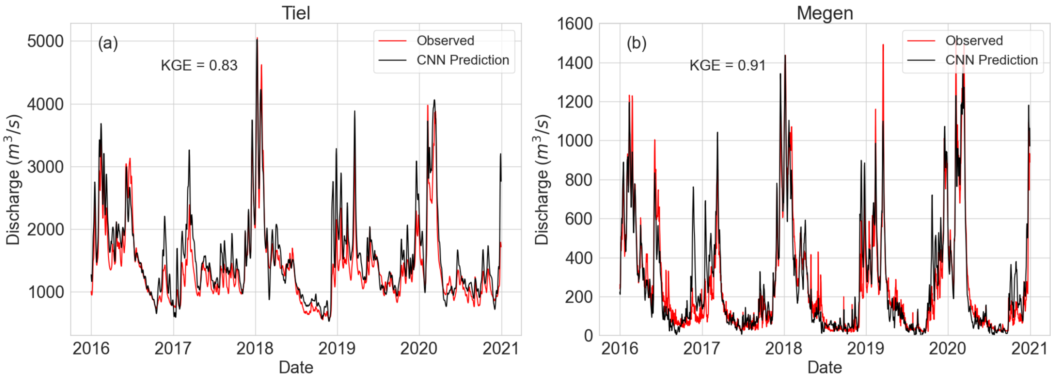

Figure 2. CNN discharge predictions compared to RWS observational record for the test period 2016-2020. The KGE is shown separately for the Tiel and Megen stations, corresponding to the Rhine and the Meuse rivers. The training period runs from 2001-2012 which is the set on which the CNN is trained. The validation period is 2013-2015, which the model has not trained on but which is used for hyperparameter and architecture tuning. The test period is from 2016-2020, which the model has not seen before the final evaluation.

horizon 2070-2100, in order to analyse the trend in SIL statistics. Particular attention is given to the high end of the spectrum, which is indicative of extreme salt intrusion events.

3 Results

3.1 CNN

The CNN is found to capture the temporal behaviour of discharge well using the variables P, T and VSW as input. Additional variables were included as CNN features but were found to either not contribute to model skill or not be available in CMIP6 output at the required spatial and/or temporal resolution. For the test period (2016 - 2020) of the ERA5 data the model predicts river discharge for the Tiel and Megen stations with a high degree of accuracy. The trends in discharge and in particular the low extremes are captured moderately well. (Supplemental Information) The KGE on the test set is 0.88 and 0.90 for the Tiel and Megen stations respectively, indicating good model performance.

When running the CNN without inclusion of the VSW variable, which would allow for a more broad selection of GCM's, the model performance drops off significantly. The performance is minimally effected by the change of spatial resolution from 0.25 to 1 degree, an adaptation which was made to fit with CMIP6 output. (Supplemental Information)

In terms of computational performance, the CNN takes 40 minutes to reach the desired level of skill over 80 epochs over training.

3.2 CMIP6 reconstructed discharge projections

Applying the CNN to CMIP forcing conditions yields a discharge time series for the entire duration of the ScenarioMIP runs, which is from 2015 to 2100. Part of the historical section of this (2015-2021) is used to evaluate the CNN's performance on the CMIP members, as opposed to its performance on ERA5 which was evaluated in the previous section. For this time frame the discharge statistics are shown as a function of the Day of Year (DOY) in Figure 3. Ensemble mean projections for the winter months are found

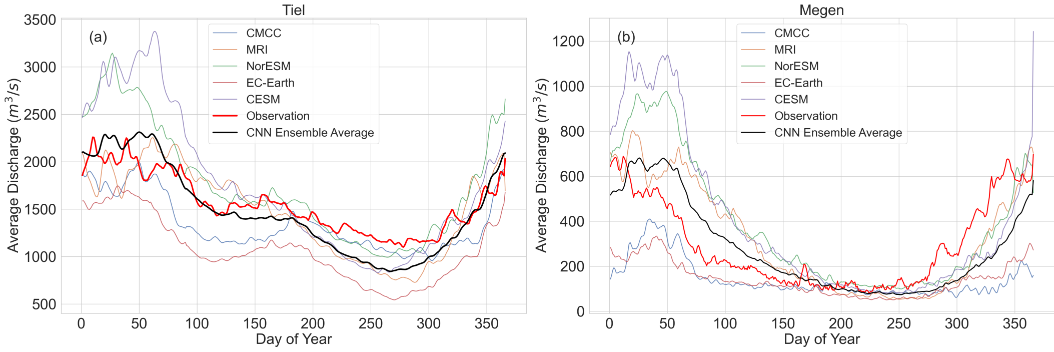

Figure 3. Seasonal discharge at the (a) Tiel and (b) Megen stations predicted by the CNN applied to the forcing output of various CMIP6 ensemble members (SSP2-4.5). The discharge values represent the average value per Day of Year (DOY) for the historical period 2015-2021. The black line shows the average measured discharge at the respective stations for the same period of time.

to correspond well to observation, but we find slight underestimation for Tiel in summer months. For Megen, order of magnitudes in river discharge are well reconstructed by the CNN model, but timing of peak is shifted by 50 days in ensemble average. Large biases can be seen here as the inter-member spread is substantially high. Due to the resemblance of the discharge bias to the bias in the forcing conditions of corresponding model runs (Supplemental Information, Figure S6), these biases are assumed to be inherent to the members themselves rather than being caused by biases in the CNN.

River discharge is projected for the entire CMIP6 time horizon 2015-2100 for the SSP2-4.5 and SSP5-8.5 scenarios and all the ensemble members included in this study. The trend in yearly 7-day minimum discharge is shown in Figure 4, where the relative difference for each year is calculated with respect to the baseline of the years 2015-2045. For the Tiel station there is no significant change in 7-day minimum discharge for the 2100 horizon in the SSP2-4.5 scenario projections, while a decrease of 5% is observed in the SSP5-8.5 scenario projections. The Megen station shows a stronger decrease in this metric as well as a large dependence on the emission scenario, with reductions of 8% and 27% for the SSP2-4.5 and SSP5-8.5 scenarios respectively. Again the inter-model spread is substantial and it can furthermore be noted that the ensemble members show future trends with a different sign. In particular, the projections based on CMCC and MRI forcing show an upward discharge trend while the projections based on the remaining three members exhibit a negative trend. This is in line with the member's future trend in mean precipitation for the RM basin, as shown in the Supplemental Information, Figure S7.

Application of the CNN to a single CMIP6 member takes 70 seconds for discharge projection of the total 2015-2100 window. Before being able to apply the CNN, data is preprocessed from a single time series to an input vector containing consecutive series of length T for each day, which takes an additional 90 seconds for each run.

3.3 Future Salt Intrusion Extremes

The time series of river discharge as obtained in the previous section are now fed into the IMSIDE model to calculate the SIL which is quantified by the 2-psu isohaline X_2. Figure 5 shows the PDF of SIL for the Nieuwe Maas for the 2015-2045 and 2070-2100 windows (a, c) as well as the difference in PDF as a function of SIL (b, d). The top and

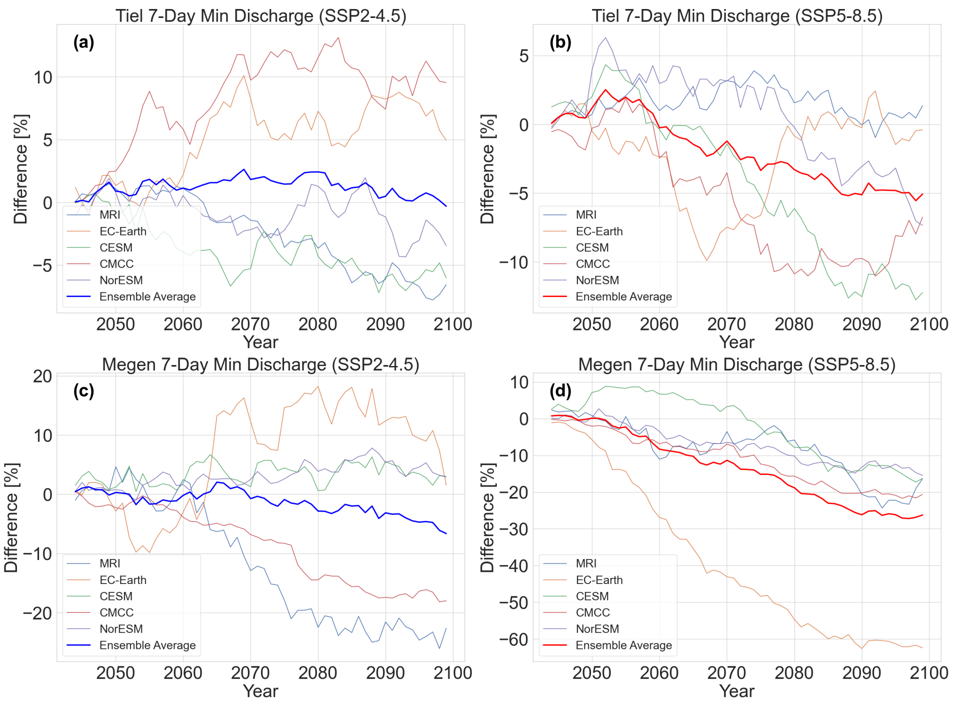

Figure 4. Deviation in yearly 7-day minimum discharge as compared to the 2015 – 2045 mean member-specific baseline. Individual calculation for CNN predictions of each of the CMIP6 ensemble members for the Tiel (a-b) and Megen (c-d) stations, SSP2-4.5 and SSP5-8.5. Ensemble averages are shown in thick lines.

bottom sub-figures correspond to the SSP2-4.5 and SSP5-8.5 runs respectively. This figure is based on IMSIDE runs where SLR is not considered.

The PDF's for the SSP2-4.5 is shown to remain relatively constant between both time windows, where little change is seen in either frequency or intensity of SI events. In particular when comparing the 2070-2100 statistics to the 2015-2045 baseline, the probability of SIL of more than 30 km increases by 1% only. For the SSP5-8.5 runs, the change is found to be significantly larger at 15% probability shift between 2070-2100 and the 2015-2045 baseline.

A shift of moderate salt intrusion events to extreme salt intrusion events is found for SSP5-8.5. The frequency of such events is projected to increase, while the intensity of the highest extremes shows little to no shift. The former can be explained by the decrease of discharge shown in the previous section (Figure 4). As discharge decreases salt intrusion events will sustain for a longer period of time (Biemond et al., 2022), causing a PDF shift towards larger X_2 as shown. The absence of a shift in the highest extremes is notable, and could be due to the increased frequency of freshwater pulses under a high emission scenario, which put a limit to the duration of salt intrusion events and therefore restrict their maximum intensity.

In terms of ensemble spread, it is clear that there is a large difference in SIL statistics between the different members (Figure 5). This is likely due to the large biases in forcing conditions present in these products. The significant positive PDF shift for the 30+ km SIL domain is however present for all ensemble members indicating a more robust outcome.

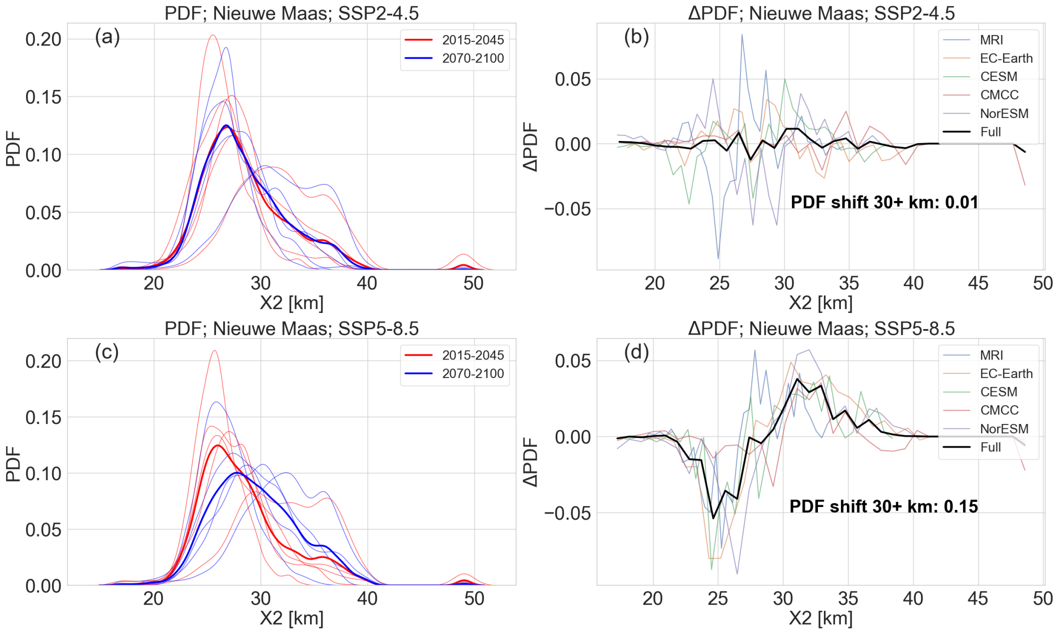

Figure 5. Comparison between periods 2015-2045 and 2070-2100 using PDF of Ensemble Average of Salt Intrusion Length in the Nieuwe Maas, for SSP2-4.5 (a-b) and SSP5-8.5 (c-d). For the former, the difference in SIL statistics between the two periods is relatively small in this case as the PDF's are close to overlapping. In SSP5-8.5, a clear change can be seen between the former and latter period where extreme salt intrusion events are more frequent and more intense.

4 Conclusion

A CNN is trained on ERA5 reanalysis data to reconstruct discharge from meteorological forcing conditions of the CMIP6 projections, and subsequently fed to IMSIDE to obtain future SIL statistics. The CNN model demonstrates strong performance in reconstructing river discharge from meteorological conditions, with KGE scores of 0.83 and 0.91 for the Rhine and Meuse rivers respectively during the test period. Application of the CNN to CMIP6 climate projections shows a 8% decrease in Rhine 7-day minimum discharge under the high emission scenario SSP5-8.5, while this parameter remains relatively constant under SSP2-4.5. The results from IMSIDE runs indicate an increase in extreme salt intrusion events in the RMD by the end of the century under the SSP5-8.5 scenario, with a projected increase of 30+ km events of 15% in the Nieuwe Maas. The moderate emission scenario SSP2-4.5 shows little to no changes which suggests a strong sensitivity of SIL to the emission pathway.

5 Discussion

This study utilizes a CNN to reconstruct discharge from meteorological forcing, as an alternative to a traditional hydrological model. While performance on the ERA5 training set is comparable to these physics-based models, its performance falls off when applied to a distinct data set (CMIP6). To illustrate this, a comparison between the CNN performance and the hydrological model wflow_sbm (van Verseveld et al., 2022) is shown in Figure 6. For both models the predicted discharge and uncertainty range for the 2016-2020 test period is shown alongside the observational record. It should be noted that the predictions are based on the KNMI'23 climate scenario's (van der Wiel et al., 2024), which utilize a different subset of CMIP6 members than the subset used in this study. The un-

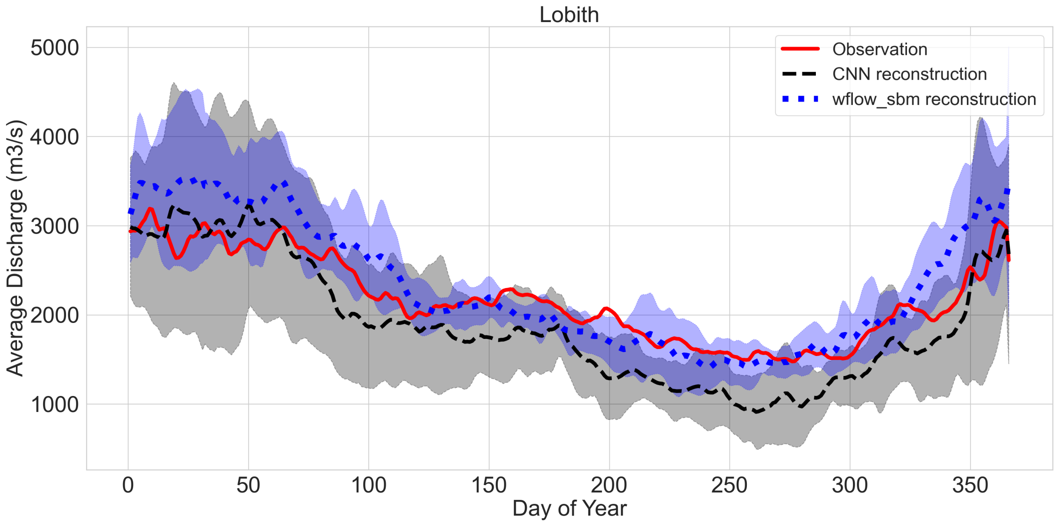

Figure 6. Comparison of the discharge reconstruction for 2015-2021 between the wflow_sbm model and the CNN used in this study, with uncertainty range σ. The Lobith station is assessed here rather than the Tiel station, as the former is used in the Deltares report considered for this comparison.

corrected time series are shown here only, as recommended for such comparative purposes (Buitink et al., 2023). Even though this is a limited time frame, wflow_sbm is shown to reconstruct discharge more accurately and with less uncertainty. While this is the expected result as the hydrological model is significantly more sophisticated, there are a number of improvements which could be made to the CNN to improve its performance on CMIP6 data.

Before considering the possible improvements to the methodology, it is important to assess the implications of these anomalies for the projected discharge and SIL results. The underestimation in summer discharge (Figure 3) has invariably influenced the subsequent CMIP6 projections, in particular when it comes to the 7-day minimum discharge displayed in Figure 4. Indeed, similar projections using the wflow_sbm model obtain a significantly larger decrease in this metric under SSP5-8.5, at 15−30% for the Rhine compared to the 5% found here. Assuming that the former is a more accurate assessment of the situation due to the more accurate model and more extensive methodology, we can conclude that the projected SIL statistics shown in this study are possibly a significant underestimation. Alternatively the absolute underestimation of summer discharge might not considerably affect the relative shift in SIL statistics presented. Furthermore, machine learning models are known to have difficulty with extreme outliers in the data. Outliers in discharge data are the cause of extreme salt intrusion events (van Den Brink et al., 2019), so this limitation might be of large influence on the SIL statistics presented here. For further research it is recommended to analyse the performance of the model on the outliers of the observational period in particular.

The presence of significant biases in forcing projections of individual ensemble members inevitably leads to similar biases in the CNN discharge output. As mentioned the driest season is where the largest errors between CNN prediction and observation occur. As the forcing itself exhibits similar biases in most models for this season (Supplemental Information), this error could likely be mitigated with proper bias correction of the input variables. It is therefore recommended to apply bias correction to the raw forcing data in further research on this approach. The aforementioned issue of a limited available time window further can complicate this process, as the bias correction would have to be based on this window 2015-2021 which is relatively small when accounting for climatological and hydrological variability.

While the CNN can relatively accurately predict river discharge based on ERA5 reanalysis data, the translation to CMIP6 application poses a number of challenges. In only using a couple of key variables as input, a lot of secondary physical effects are disregarded in this analysis. The contribution of these secondary effects might be consistent within the ERA5 reanalysis framework and for the relatively short-term period 2001-2020, but this need not be the case for CMIP6 projections up to 2100. The current analysis could be improved by increasing the training and test period, as reanalysis data is available from the ERA5 dataset starting in 1990. There are also a number of additional variables which may improve model skill, like wind speed, which are included in both the ERA5 reanalysis product as well as the ScenarioMIP projections for the relevant temporal and spatial resolution, and therefore could be added to the CNN setup.

Taking a broader look at the salt intrusion phenomenon, sea level rise is found to be a dominant effect on SIL in studies on the RMD (van Den Brink et al., 2019) but it is not within the scope of this study. Tentative simulations have however been carried out where the effect of SLR included, by increasing the depth of each channel in IMSIDE with a fixed amount. (Supplemental Information) The results indicate that SLR has a significantly stronger effect on SIL than the discharge reduction considered in the main results of this study. It should be noted however that it is difficult to compare the two effects in this manner. The effect of discharge is quantified by an extensive process starting from projected forcing conditions from different members where many uncertainties influence the SIL statistics. The straightforward approach of adding depth to each channel contains less of such uncertainties, while at the same time being less precise as the SLR is only induced with a single fixed value rather than a gradual increase of sea level. Combining these considerations with the extrapolation issues of the CNN to CMIP6 discussed previously, we do not draw conclusions on the comparative importance of SLR and discharge reduction on RMD salt intrusion from this study.

The machine learning approach presented here benefits greatly from a very cheap computational cost as well as a flexible application framework. The discharge reconstruction component of the current analysis can be readily extrapolated to any river in the world where an observational record of discharge is available. By going through the process of training on ERA5 data and applying to CMIP6 data, time series of future river discharge can be obtained in quick fashion. In particular such river discharge data could serve as an alternative to the discharge currently provided in model projections, as the station-specific discharge could be more relevant for practical water management applications than the cell-based discharge commonly found in raw model output. Furthermore it is recommended to apply the CNN to ensemble runs of individual models in order to gain understanding of the internal variability of the GCM's themselves.

Open Research

Historical discharge data used for training the model is obtained from Rijkswaterstaat. (Rijkswaterstaat, 2024) Reanalysis data from ERA5 is used to construct the input vector. (Hersbach et al., 2020) CMIP data is obtained from ScenarioMIP output. The IMSIDE model is publicly available. (Biemond et al., 2022)

Acknowledgments

This research was carried out as a part of the SALTIsolutions project, which tackles the threatened availability of fresh water in the Rhine-Meuse Delta due to Saltwater Intrusion. The SALTIsolutions is financed by NWO Domain Applied and Engineering Sciences. (NWO, 2024)

I would like to thank my supervisor Henk Dijkstra for his support and valuable feedback during the course of this project. I would also like to give special thanks to Jiyong Lee who helped me with the methodology of this project and provided great feedback throughout on the approach, the evaluation and the presentation of the research. I want to thank Bouke van Biemond for allowing the use of IMSIDE and helping with its setup, as well as providing valuable feedback on the project and the thesis.

References

Bellafiore, D., Ferrarin, C., Maicu, F., Manfè, G., Lorenzetti, G., Umgiesser, G., … Levinson, A. V. (2021). Saltwater intrusion in a mediterranean delta under a changing climate. *Journal of Geophysical Research: Oceans*, *126*(2), e2020JC016437.

Biemond, B., de Swart, H. E., & Dijkstra, H. A. (2023). Mechanisms of salt overspill at estuarine network junctions explained with an idealized model. *Journal of Geophysical Research: Oceans*, *128*(3), e2023JC019630.

Biemond, B., de Swart, H. E., Dijkstra, H. A., & Díez-Minguito, M. (2022). Estuarine salinity response to freshwater pulses. *Journal of Geophysical Research: Oceans*, *127*(11), e2022JC018669.

Biemond, B., Vuik, V., Lambregts, P., de Swart, H. E., & Dijkstra, H. A. (2024). Salt intrusion and effective longitudinal dispersion in man-made canals, a simplified model approach. *Estuarine, Coastal and Shelf Science*, *298*, 108654.

Buitink, J., Tsiokanos, A., Geertesma, T., Ten Velden, C., Bouaziz, L., & Sperna Weiland, F. (2023). *Implications of the knmi'23 climate scenarios for the discharge of the rhine and meuse* (Tech. Rep.). Deltares.

Chen, S.-N. (2015). Asymmetric estuarine responses to changes in river forcing: A consequence of nonlinear salt flux. *Journal of Physical Oceanography*, *45*(11), 2836–2847.

Dadson, S., Bell, V., & Jones, R. (2011). Evaluation of a grid-based river flow model configured for use in a regional climate model. *Journal of hydrology*, *411*(3-4), 238–250.

Danabasoglu, G., Lamarque, J.-F., Bacmeister, J., Bailey, D., DuVivier, A., Edwards, J., … others (2020). The community earth system model version 2 (cesm2). *Journal of Advances in Modeling Earth Systems*, *12*(2), e2019MS001916.

de Nijs, M. A., & Pietrzak, J. D. (2012). Saltwater intrusion and etm dynamics in a tidally-energetic stratified estuary. *Ocean Modelling*, *49*, 60–85.

Döscher, R., Acosta, M., Alessandri, A., Anthoni, P., Arneth, A., Arsouze, T., … others (2021). The ec-earth3 earth system model for the climate model intercomparison project 6. *Geoscientific Model Development Discussions*, *2021*, 1–90.

Garner, G., Hermans, T. H., Kopp, R., Slangen, A., Edwards, T., Levermann, A., …

others (2022). Ipcc ar6 wgi sea level projections.

Hauswirth, S. M., Bierkens, M. F., Beijk, V., & Wanders, N. (2021). The potential of data driven approaches for quantifying hydrological extremes. *Advances in Water Resources*, *155*, 104017.

Hersbach, H., Bell, B., Berrisford, P., Hirahara, S., Horányi, A., Muñoz-Sabater, J., . . . others (2020). The era5 global reanalysis [dataset]. *Quarterly Journal of the Royal Meteorological Society*, *146*(730), 1999–2049.

Huismans, Y., Kuijper, C., Kranenburg, W., de Goederen, S., Haas, H., & Kielen, N. (2017). Predicting salinity intrusion in the rhine-meuse delta and effects of changing the river discharge distributions. *Netherlands Centre for River Studies*.

Jacobs, P., Blom, G., & van der Linden, T. (2000). Keynote paper 2 climatological changes in storm surges and river discharges: the impact on flood protection and salt intrusion in the rhine-meuse delta. *ECLAT-2*, 35.

Klijn, F., van Velzen, E., ter Maat, J., Hunink, J., Baarse, G., Beumer, V., . . . others (2012). *Zoetwatervoorziening in nederland: aangescherpte landelijke knelpuntenanalyse 21e eeuw* (Tech. Rep.). Deltares.

Knoben, W. J., Freer, J. E., & Woods, R. A. (2019). Inherent benchmark or not? comparing nash–sutcliffe and kling–gupta efficiency scores. *Hydrology and Earth System Sciences*, *23*(10), 4323–4331.

Lee, J., Biemond, B., de Swart, H., & Dijkstra, H. A. (2024). Increasing risks of extreme salt intrusion events across european estuaries in a warming climate. *Communications Earth & Environment*, *5*(1), 60.

Lovato, T., Peano, D., Butenschön, M., Materia, S., Iovino, D., Scoccimarro, E., . . . others (2022). Cmip6 simulations with the cmcc earth system model (cmcc-esm2). *Journal of Advances in Modeling Earth Systems*, *14*(3), e2021MS002814.

M. dörrbecker. (2019). Retrieved from `https://commons.wikimedia.org/w/index.php?curid=46754100`

Monismith, S. G., Kimmerer, W., Burau, J. R., & Stacey, M. T. (2002). Structure and flow-induced variability of the subtidal salinity field in northern san francisco bay. *Journal of physical Oceanography*, *32*(11), 3003–3019.

NWO. (2024). *Saltisolutions.* https://www.nwo.nl/onderzoeksprogrammas/perspectief/perspectief-toekenningen/saltisolutions. ([Online; accessed 18-April-2024])

O'Neill, B. C., Tebaldi, C., Van Vuuren, D. P., Eyring, V., Friedlingstein, P., Hurtt, G., . . . others (2016). The scenario model intercomparison project (scenariomip) for cmip6. *Geoscientific Model Development*, *9*(9), 3461–3482.

Pereira, H., Sousa, M. C., Vieira, L. R., Morgado, F., & Dias, J. M. (2022). Modelling salt intrusion and estuarine plumes under climate change scenarios in two transitional ecosystems from the nw atlantic coast. *Journal of Marine Science and Engineering*, *10*(2). Retrieved from `https://www.mdpi.com/2077-1312/10/2/262`

Qiao, L., Zuo, Z., & Xiao, D. (2022). Evaluation of soil moisture in cmip6 simulations. *Journal of Climate*, *35*(2), 779–800.

Rijkswaterstaat. (2024). *Historical water data* [dataset]. https://rijkswaterstaatdata.nl/waterdata/. ([Online; accessed 10-March-2024])

Savenije, H. (2012). *Salinity and tides in alluvial estuaries* (2nd ed.). Delft.

Seland, Ø., Bentsen, M., Olivié, D., Toniazzo, T., Gjermundsen, A., Graff, L. S., . . . others (2020). Overview of the norwegian earth system model (noresm2) and key climate response of cmip6 deck, historical, and scenario simulations. *Geoscientific Model Development*, *13*(12), 6165–6200.

Sun, D., Wu, J., Huang, H., Wang, R., Liang, F., & Xinhua, H. (2021). Prediction of short-time rainfall based on deep learning. *Mathematical Problems in Engineering*, *2021*, 1–8.

Tran, D., Bourdev, L., Fergus, R., Torresani, L., & Paluri, M. (2015). Learning spatiotemporal features with 3d convolutional networks. In *Proceedings of the ieee international conference on computer vision* (pp. 4489–4497).

Uehlinger, U. F., Wantzen, K. M., Leuven, R. S., & Arndt, H. (2009). The rhine river basin.

van Den Brink, M., Huismans, Y., Blaas, M., & Zwolsman, G. (2019). Climate change induced salinization of drinking water inlets along a tidal branch of the rhine river: Impact assessment and an adaptive strategy for water resources management. *Climate*, *7*(4), 49.

van der Wiel, K., Beersma, J., van den Brink, H., Krikken, F., Selten, F., Severijns, C., ... van Dorland, R. (2024). Knmi'23 climate scenarios for the netherlands: Storyline scenarios of regional climate change. *Earth's Future*, *12*(2), e2023EF003983.

van Verseveld, W. J., Weerts, A. H., Visser, M., Buitink, J., Imhoff, R. O., Boisgontier, H., ... others (2022). Wflow_sbm v0. 6.1, a spatially distributed hydrologic model: from global data to local applications. *Geoscientific Model Development Discussions*, *2022*, 1–52.

Wullems, B. J., Brauer, C. C., Baart, F., & Weerts, A. H. (2023). Forecasting estuarine salt intrusion in the rhine–meuse delta using an lstm model. *Hydrology and Earth System Sciences*, *27*(20), 3823–3850.

Yukimoto, S., Kawai, H., Koshiro, T., Oshima, N., Yoshida, K., Urakawa, S., ... others (2019). The meteorological research institute earth system model version 2.0, mri-esm2. 0: Description and basic evaluation of the physical component. *Journal of the Meteorological Society of Japan. Ser. II*, *97*(5), 931–965.

Supplemental Information

A) CNN Setup and Tuning

General Approach

As we are considering the discharge statistics, the CNN must predict the daily discharge value in m^3s^{-1} at the Tiel and Megen stations for the Rhine and Meuse rivers respectively. The model will make its prediction based on time series of spatial maps of meteorological variables. It is clear that it will not be enough to use spatial or temporal averages of these variables. Large anomalies in precipitation in the Alps will not be felt in terms of station discharge instantaneously, but its effects will be delayed for weeks. Similarly, the precipitation just a few kilometers upstream of Tiel will be relevant for the discharge value of the same or the next day. However, this same precipitation value will not be relevant for the discharge of weeks to come. Clearly, the spatiotemporal component of our data is crucial and must not be negated by taking averages over either time or space.
The time-series of each variable and its locations must be preserved in order for the model to obtain the required skill.

Variables and Resolution

Tuning of the CNN in the scope of this research concerns primarily the spatial resolution of the input vector, as well as the input variables included in the model. The model was initially trained on 0.25 degree resolution as this is the available resolution from the ERA5 product. ERA5 also has finer output such as ERA5-LAND, but the 0.25 degree was chosen as a starting point based on weighing the added value of a finer resolution to the associated increase in computational cost. The model was eventually adjusted to require a 1 degree resolution, as this matches the output resolution of the ScenarioMIP product. The selection of input variables is complicated especially due to the need to have matching variables in the future projections on which the trained CNN is applied. The KNMI'23 Climate Scenario's are a great fit for this research since they provide climate projections on a daily scale based on scenario's selected specifically for the Netherlands, as well as the inclusion of the entire RM basin in its output (van der Wiel et al., 2024). Crucially though these projections do not include a variable representing the soil moisture content.
To decide if this is a bottleneck for CNN performance, and how it compares to the increased performance of better resolution (which KNMI'23 would provide), many validation runs of the CNN were done using different variables and spatial resolution. Figure S1 shows the comparative performance in the validation set (2013-2015) for 4 such setups, where the resolution is either 0.25 or 1 degrees and where the soil moisture content VSW is included or excluded. It is concluded that the inclusion of the VSW variable improves model performance significantly, regardless of the spatial resolution of the input features. Improving the spatial resolution brings a relatively small performance benefit in comparison. Furthermore, the choice for a machine learning solution for the discharge reconstruction lies in part in the computational benefits that such a solution provides. The spatial resolution largely determines the computation time for machine learning models (Tran et al., 2015), and choosing the 0.25 degree route would hamper the learning time significantly. Based on these considerations we decided to use the 1 degree model in combination with the CMIP6 climate projections, with inclusion of the VSW variable.

Input Vector

The CNN works on input samples which each consist of a time series of maps for each of the considered meteorological variables. We can think of these samples as being videos

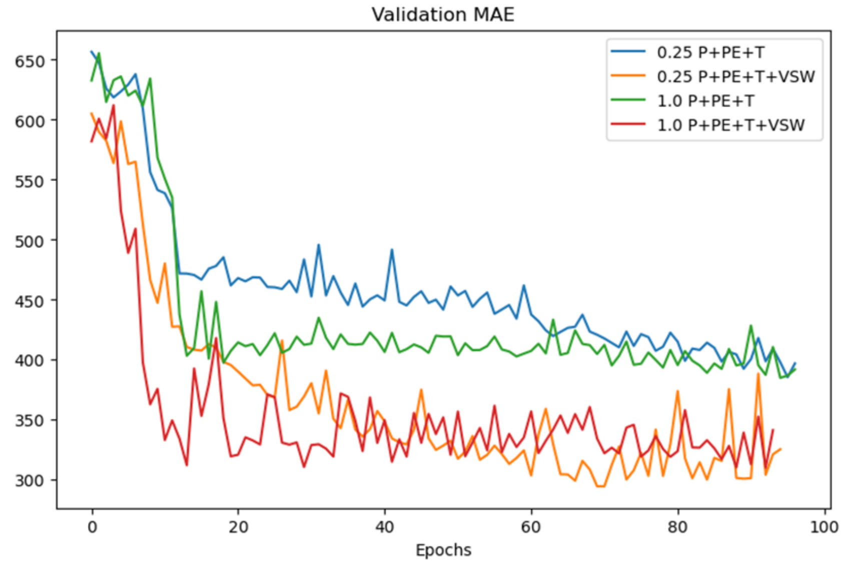

Figure S1. Mean absolute error (MAE) of discharge for the validation set (2013-2015) as a function of training epoch. The CNN setup is varied between spatial resolution of 0.25 and 1 degree as well as whether the soil moisture variable VSW is included.

of the basin area over the entirety of the lead time. Each sample is therefor a 4D array of the following shape: (x, y, t, D). Here x and y are the amount of grid cells in longitudinal and latitudinal direction, respectively. t represents the amount of time steps in a single sample, which is equal to the amount of days the input video lasts. D represents the amount of different input variables considered. For most of the model runs, the first three of these will be kept constant. The dimensionality D will be varied a lot to investigate the relative predictive value of each input variable in detail. When feeding the input to our CNN model, the input vector is extended to a 5D array to include the amount of training samples, denoted by N. Such that the input vector becomes (N, x, y, t, D).

Preprocessing

ERA5 data is obtained in hourly frequency. The data is resampled to daily averages for T and VSW and a daily sum for P. The considered latitude range is $(46, 53)$ while the longitude range is $(3, 12)$. This corresponds to a somewhat extensive square around the relevant (upstream of Tiel and Megen) sections of the Rhine/Meuse basin. Even in this area there are of course many grid cells that are far from the actual Rhine river or even any river branches. The meteorological data for these grid cells is not relevant to the discharge prediction. Given a long enough time to train, the machine learning approach will eliminate this problem by itself, as the model will pick up on the irrelevance of the data in these grid cells to the output variable and adjusted the corresponding weights accordingly. However this might unnecessarily increase the duration of the learning process, especially since there will be a lot of auto-correlation present between relevant and irrelevant grid cells. Therefore the model's life is made a bit easier by applying a mask over the irrelevant areas.
Next, the daily data is transformed to an input vector in the following way. For each day in the considered period, the data of the relevant time window is aggregated into a single array. This array represents all the input data of the single sample. This is repeated for each day contained in the time period to produce the input vector. Each sample can be viewed as a series of videos of the considered variables over time.

Layers	Input	Output	Kernel size	Activation
Conv3D	3	16	(1, 2, 2)	ReLU
Conv3D	16	16	(5, 1, 1)	ReLU
Conv3D	16	16	(1, 2, 2)	ReLU
Conv3D	16	16	(5, 1, 1)	ReLU
Flatten	16	x	-	-
Dense	X	128	-	ReLU
Dense	128	64	-	ReLU
Dense	64	32	-	ReLU
Dense	32	16	-	ReLU
Dense	16	1	-	ReLU

Table 2. Complete architecture of the CNN. After the last Conv3D layer the channels are flattened to obtain an output of dimension 1 and length X (the X depends of the input vector).

The data is normalized for each variable separately before being fed into the ML model.

CNN architecture

The input vector obtained through preprocessing serves as the input for the CNN model. The output (labels) are now the river discharge values. The model uses 3D convolutional layers, which apply convolutional operators in the spatial and temporal dimension. As demonstrated in (Tran et al., 2015), splitting up the 3D filters into distinct spatial and temporal components provides significantly gains in accuracy as well as computation speed. Therefore the convolutional is first applied in spatial dimension only and consequently applied in temporal dimension only. This is represented in the architecture overview (Table 2 as the (1, 2, 2) and (5, 1, 1) kernel size, respectively. The spatial kernel is small as the total grid representing the Rhine basin is 9x9 grid points only. This is also the reason why MaxPooling layers are not included in the model. The temporal size of the input vector is larger at 40 days for the Rhine basin, allowing for a larger kernel in this dimension. Following two sets of convolutional hidden layers a flattening layer is applied, and finally the CNN has 5 dense layers before producing the discharge prediction. Each layer utilizes the ReLU activation function as the

Determination of Time Delay

To determine the length of the input vector in terms of the amount of lead days, the correlation between precipitation and measured river discharge is calculated as a function of the lead time. The purpose of this calculation is to determine how far in advance the basin-wide meteorological factors start to influence the river discharge at the relevant downstream measurement station. For example, an extreme precipitation event in the Alps will only be reflected in the river discharge in the Netherlands after multiple weeks at least. The size of the time delay is a trade-off: a larger window will ensure that these delayed responses are captured which can be crucial for the Rhine basin especially. A smaller window is also advantageous as a smaller input vector will decrease computational cost. It can furthermore be detrimental to the convergence time of the CNN if the time delay is too large and the input vector therefore contains more relatively insignif-

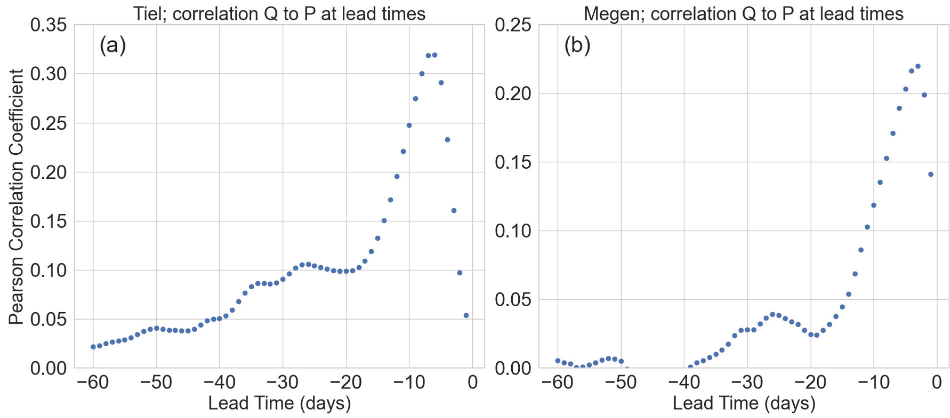

Figure S2. Correlation coefficient of ERA5 basin-wide precipitation and measured river discharge at the (a) Tiel and (b) Megen stations, as a function of lead time. Amount of days of the x-axis represents the amount of days that the precipitation statistics predate the river discharge data.

icant features. The results of this analysis are shown in Figure S2 for the Tiel and Megen stations. Based on the aforementioned arguments, the lead times were set at 40 days for Tiel and 20 days for Megen.

B) Additional Figures

Oude Maas SIL statistics

The PDF of the SIL X_2 for the baseline period 2015-2045 as well as the future horizon 2070-2100 are presented in Figure S3, for SSP2-4.5 and SSP5-8.5 runs. As in the Nieuwe Maas SIL statistics presented in the main text, there is little to no change in the PDF for the SSP2-4.5 runs. Again a significant positive signal is found for the SI events in the SSP5-8.5 scenario, where the 30+ km events increase by 15%.

SIL statistics including SLR

IMSIDE provides a means to estimate the effect of SLR on the SIL statistics by increasing the depth of each of the river channels by a fixed amount. Using SLR projections from NASA based on the AR6 climate scenarios (Garner et al., 2022), estimations for SLR by 2085 were found to be $0.49m$ and $0.61m$ for SSP2-4.5 and SSP5-8.5 respectively (Maassluis station). The effect of SLR on SIL statistics is considered by including separate IMSIDE runs where this SLR is taken into account by increasing the depth of each river channel with the stated amounts. It should be noted that the discharge input is kept the same as the previous runs such that these results represent the combined effect of SLR and discharge reduction.

Here the X_2 PDF obtained from IMSIDE runs where the effect of SLR is included are shown. SLR is induced by increasing the depth setting of each channel in the RMD in the IMSIDE geological model. The SLR is prescribed as a constant rather than a time series as the latter is not supported in IMSIDE. To evaluate the SIL statistics, the 2070-2100 statistics from the SLR runs are compared to the 2015-2045 statistics from the baseline (no SLR) runs. All runs use the CNN-projected discharge as primary forcing input.

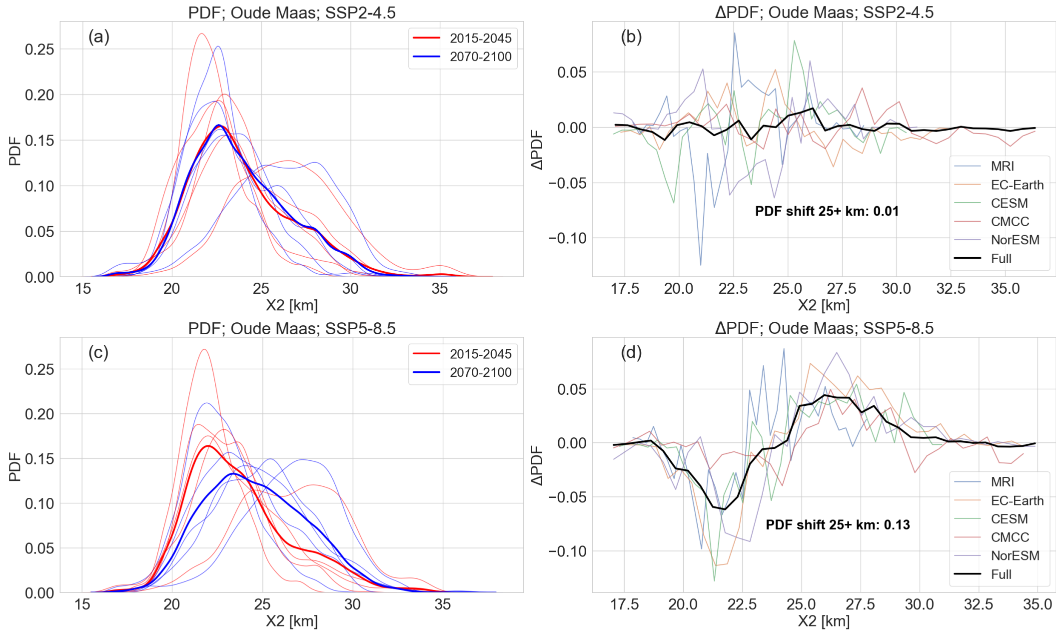

Figure S3. Comparison between time windows 2015 − 2045 and 2070 − 2100 using PDF of Ensemble Average of SIL in the Oude Maas, for SSP2-4.5 (a-b) and SSP5-8.5 (c-d). (ASO only) For the former, the difference in SIL statistics between the two periods is relatively small in this case as the PDF's are close to overlapping. In SSP5-8.5, a clear change can be seen between the former and latter period where extreme salt intrusion events are more frequent and more intense.

The SLR values are obtained from the AR6 based NASA SLR tool (Garner et al., 2022), linearly interpolated to the year 2085 for the Maassluis site.

The results of these simulations are shown in Figures S4 and S5 for the Nieuwe Maas and the Oude Maas respectively. When compared to the runs without SLR in the main text, the PDF shift is significantly more present here. The PDF shift in the SSP5-8.5 scenario is 36% and 42% for the Nieuwe Maas and Oude Maas, compared to the 13% and 15% increase in the runs without SLR. Additionally, the SLR runs show an increase of 17% and 24% for the SSP2-4.5 scenario, where a significantly increase was absent in the runs without SLR.

CMIP6 Climate Variable Time Series

In the CNN-predicted discharge based on the CMIP6 data, large biases are observed with respect to the corresponding historical discharge measured at the downstream stations. These biases in discharge are assumed to be a direct result of biases in the forcing of the individual CMIP6 members. To illustrate this, Figure **??** shows the DOY means of each variable for the historical period 2015-2021 with a comparison to the ERA5 means for the same period. Indeed, the biases observed in the precipitation and volumetric soil moisture especially reflect well the biases seen in the river discharge predictions by the CNN (Figure 3).

In addition to the comparison in the historical period, it is also imperative to consider the temporal trends in forcing conditions for each of the CMIP6 ensemble members. For this purpose a baseline is calculated for each member and variable separately based on the first 20 year of the time series. The relative difference of yearly mean forcing values

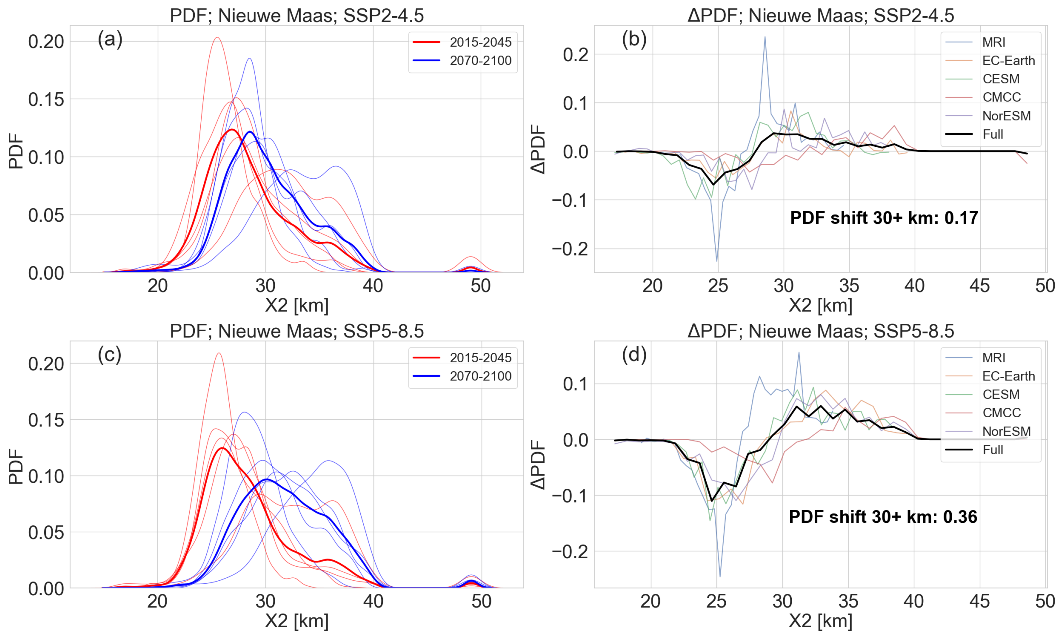

Figure S4. Same as Figure 5 where the effect of SLR is taken into account in the IMSIDE runs. (ASO only)

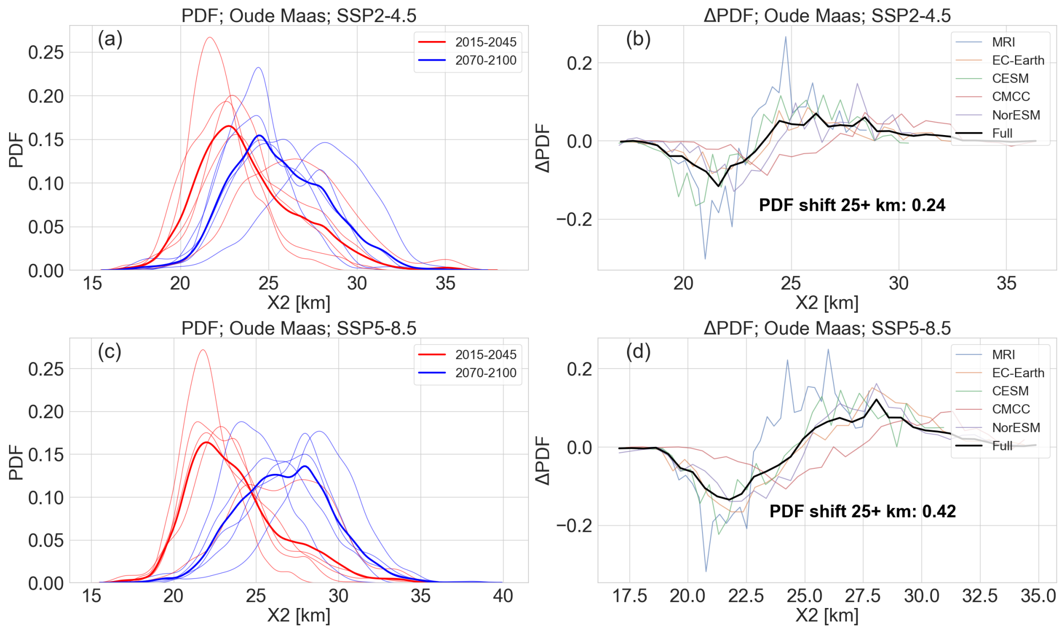

Figure S5. Same as Figure 5 where the effect of SLR is taken into account in the IMSIDE runs. (ASO only)

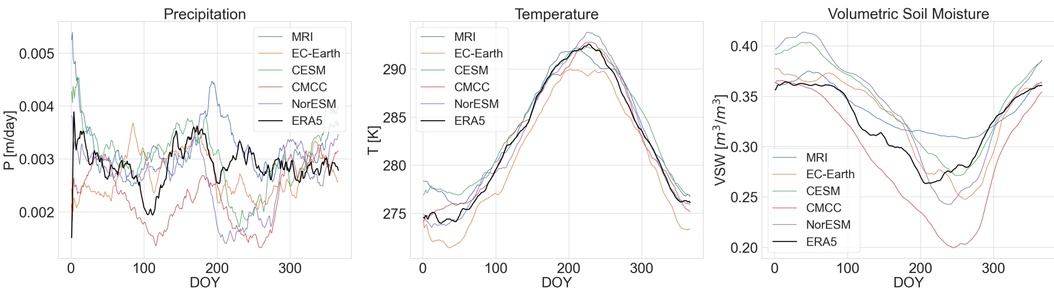

Figure S6. Climate variable means per Day of Year (DOY) for the historical period 2015-2021, with a comparison to the DOY mean in the reanalysis set ERA5. This plot is meant to illustrate the biases present in the individual CMIP6 members, and serves as comparison to the discharge biases shown in Figure 3. The averages are calculated over the entire region of the Rhine-Meuse Basin.

is then compared to this baseline to illustrate the temporal evolution, shown in Figure S7. The trends in this analysis are to be compared to the trends seen in the CNN-predicted time series of yearly 7-day minimum discharge for the corresponding CMIP6 ensemble members (Figure 4).

C) IMSIDE Model

A comprehensive overview of the IMSIDE model used for SIL prediction is given her. For more detailed analysis, please refer to publications on this model, (Biemond et al., 2022, 2023, 2024).

IMSIDE utilizes the salt conservation equation as follows:

$$\frac{\partial s}{\partial t} + \frac{1}{b}\frac{\partial}{\partial x}(bus) + \frac{\partial}{\partial z}(ws) = \frac{1}{b}\frac{\partial}{\partial x}(bK_h\frac{\partial s}{\partial x}) + \frac{\partial}{\partial z}(K_v\frac{\partial s}{\partial z}) \tag{1}$$

In this equation, s is the salinity, b is the width of the estuary, u is the (horizontal) flow velocity, w is the vertical velocity, and K_h, K_v are the parameterized horizontal and vertical eddy diffusivity. x and z represent the horizontal (along-channel) and vertical dimensions while t is the time.

Since salt intrusion in estuaries is highly dependent on depth-varying density and concentration differences, the model is depth-resolving rather than depth-averaged. To achieve this, both flow velocity and salinity are split into a depth-averaged and a depth-dependent component as follows:

$$u = \bar{u} + u', \quad s = \bar{s} + s' \tag{2}$$

Combining Equations 1 and 2 yields the depth-averaged salt balance as follows:

$$\frac{\partial \bar{s}}{\partial t} + \frac{1}{b}\frac{\partial}{\partial x}(b\bar{u}\bar{s}) + \frac{1}{b}\frac{\partial}{\partial x}(b\overline{u's'}) - \frac{1}{b}\frac{\partial}{\partial x}(bK_h\frac{\partial s}{\partial x}) \tag{3}$$

Here the dominant terms of the flux balance between downstream and upstream directed processes are transparently represented. The second term represents the downstream freshwater discharge pushing the saline water back in the seaward direction. The third term

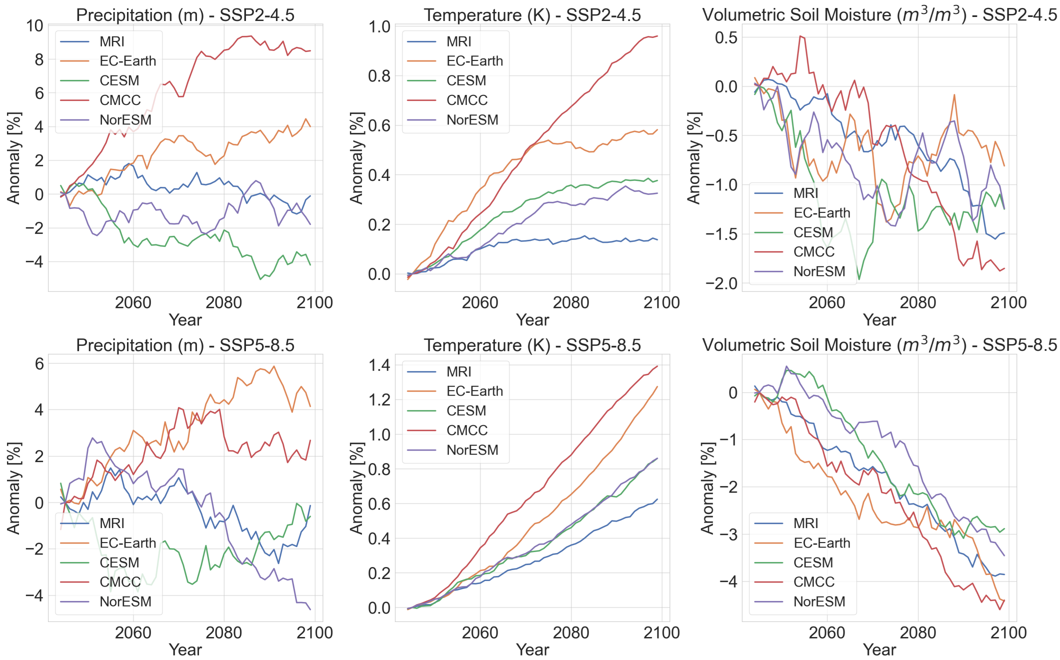

Figure S7. Deviation in the three considered variables P, T and VSW as compared to the $2015-2045$ baselines. Individual calculation for each of the CMIP6 ensemble members for SSP2-4.5 and SSP5-8.5. The averages are calculated over the entire region of the Rhine-Meuse Basin.

captures the upstream processes, which include the effect of the density-driven estuarine circulation as well as a contribution induced by the river current. The final term represents the horizontal diffusive flux, which can be an upstream or a downstream contribution based mainly on the phase coupling of flow velocity and salinity. The temporal evolution of the depth-averaged salinity is obtained by solving for the first term. To obtain evolution of the depth-dependent salinity s', Equation 3 is subtracted from 1 (not shown). A Galerkin method is used to deal with vertical variations.